Temperature dependence of the Kirkwood correlation factor and linear dielectric constant of simple isotropic polar fluids

Pierre-Michel Déjardin,[1] Florian Pabst,[2] Yann Cornaton,[3] Andreas Helbling,[2] and Thomas Blochowicz[2]

[1]*Laboratoire de Modélisation Pluridisciplinaire et Applications, Université de Perpignan Via Domitia, 52 avenue Paul Alduy, F-66860 Perpignan, France*

[2]*Institute of Condensed Matter Physics, Technische Universität Darmstadt, D-64289 Darmstadt, Germany*

[3]*Laboratoire de Chimie Systémique Organo-Métallique, Institut de Chimie de Strasbourg, Université de Strasbourg, F-67000 Strasbourg*

(Received 6 December 2021; accepted 24 January 2022; published 8 February 2022)

The theory developed in an accompanying paper [Déjardin, Phys. Rev. E **105**, 024109 (2022)] is used to compute the Kirkwood correlation factor of simple polar fluids of different nature. From this calculation, the theoretical static permittivity is readily obtained, which is compared with experimental values. This is accomplished by fitting only one parameter accounting for induction or dispersion forces and torques, which is necessarily connected with the individual molecular polarizability but not explicitly related to the physical properties due to the nonadditivity of such energies. Excellent agreement between theoretical and experimental static permittivities is obtained over a very broad temperature range for a number of associated and nonassociated liquids. Finally, limitations of the present theory are given.

DOI: 10.1103/PhysRevE.105.024108

I. INTRODUCTION

The theory of the linear dielectric constant of isotropic polar fluids was initiated by Debye nearly a century ago [1]. By its simplicity, Debye's theory is *qualitatively* sufficient to describe the temperature dependence of the dielectric constant of polar fluids. However, it is nowadays recognized that Debye's theory strictly applies to very dilute systems only, because either in its Debye-Langevin version or in its Debye-Lorentz one [2,3], *quantitative* disagreement between theory and experiment arises as a result of both poorly representing the local field *and* not accounting for intermolecular interactions at the statistical-mechanical level.

Onsager's theory [4] allows one to remove the ferroelectric Curie point arising from the Debye-Lorentz theory. However, for many substances (mainly associated liquids), Onsager's theory leads to a temperature-dependent individual molecular dipole, which is inconsistent with, e.g., *ab initio* quantum-mechanical calculations of the dipole moment of an isolated molecule. Kirkwood and Fröhlich [5,6] included intermolecular interactions into Onsager's calculation, resulting in the Onsager-Kirkwood-Fröhlich (nowadays termed Kirkwood-Fröhlich) theory. It simply consists in replacing the square modulus of the molecular dipole μ^2 in Onsager's theory by $\mu^2 g_{\mathrm{K}}$, where g_{K} is Kirkwood's correlation factor, which accounts for pair dipolar ordering in the substance under consideration. This results in the equation commonly used to experimentally determine the Kirkwood correlation factor from dielectric measurements:

$$g_{\mathrm{K}} = \frac{9\varepsilon_0 kTM_{\mathrm{mol}}}{\mu_g^2 N_A M_v(T)} \frac{(\varepsilon-\varepsilon_\infty)(2\varepsilon+\varepsilon_\infty)}{\varepsilon(\varepsilon_\infty+2)^2}, \tag{1}$$

where k is Boltzmann's constant, T the absolute temperature, ε_0 the permittivity of vacuum, M_{mol} the molecular weight, μ_g the molecular dipole moment in the ideal gas phase, N_A Avogadro's number, $M_v(T)$ the mass density, and ε and ε_∞ the static and high-frequency permittivities, respectively. A molecular expression for g_{K} was derived by Fröhlich [7] in terms of mean cosines of the angle between pairs of molecules $\langle\cos\vartheta_{1j}\rangle$, *viz.,* ($\mathbf{u}_i$ denotes the orientation of the dipole of molecule i and $\cos\vartheta_{ij} = \mathbf{u}_i\cdot\mathbf{u}_j$, and the angular brackets $\langle\rangle$ denote an equilibrium average in the absence of externally applied fields)

$$g_{\mathrm{K}} = 1 + \sum_{j\neq 1}\langle \mathbf{u}_1\cdot\mathbf{u}_j\rangle = 1 + \sum_{j\neq 1}\langle\cos\vartheta_{1j}\rangle, \tag{2}$$

so that the g_{K} values deduced from experimental data are customarily compared with unity in order to determine whether the dipole moments tend to align parallel or antiparallel. More precisely, the rule of thumb is such that if $g_{\mathrm{K}} > 1$, then $\langle\cos\vartheta_{1j}\rangle$ is essentially positive, so that pairs of dipoles have a trend to orient parallel, while $g_{\mathrm{K}} < 1$ implies a trend to orient antiparallel, as $\langle\cos\vartheta_{1j}\rangle$ is essentially negative. However, it will be shown below that this crude picture is an oversimplification and therefore should be used with caution.

Despite an enormous theoretical effort that was made especially in the 1970s and 1980s in order to theoretically compute g_{K} [8–12], the so-deduced g_{K} values did not allow to reproduce the *experimentally deduced* values of the Kirkwood correlation factor at each temperature, and therefore, the aforementioned theoretical results are not, strictly speaking, amenable to *quantitative* comparison with experimental data. This is the reason why the theory of the dielectric constant was reconsidered [13] in order to provide g_{K} values which

can be *quantitatively compared with experimental ones*. The aim of this paper is to check whether this is indeed the case. Therefore, after summarizing the basic theoretical results in the next section, the dependence of the calculated g_K values on the different parameters of the theory are visualized in order to get a feeling for the behavior of the equations. We will assume, following Debye [1], that the dipole moment is along the long symmetry axis of thin rod (or symmetric top) -shaped molecules for simplicity, so that the orientation of a molecule is that of the molecular dipole. Then the theoretical values of the static permittivity are compared with the experimental ones for various liquids with preferred parallel and antiparallel ordering.

II. THEORETICAL BACKGROUND

A. Summary of the theoretical results

In a companion paper [13], one of us has derived an integral formula for the Kirkwood correlation factor of polar fluids in terms of the equilibrium pair orientational probability density $W_2^{(0)}(\mathbf{u}_1, \mathbf{u}_2)$ that a pair of interacting dipoles numbered 1 and 2 have orientations $(\mathbf{u}_1, \mathbf{u}_2)$ at thermal equilibrium. This formula is

$$g_K = 1 - \frac{2\beta}{3} \int \nabla_{\mathbf{u}_1} U_m^{\infty}(\mathbf{u}_1, \mathbf{u}_2) \cdot \Big\{ \nabla_{\mathbf{u}_1} P_2(\mathbf{u}_1 \cdot \mathbf{e}) + \frac{9}{4} \nabla_{\mathbf{u}_1} [(\mathbf{u}_1 \cdot \mathbf{e})(\mathbf{u}_2 \cdot \mathbf{e})] \Big\} W_2^{(0)}(\mathbf{u}_1, \mathbf{u}_2)\, d\mathbf{u}_1\, d\mathbf{u}_2, \quad (3)$$

where $\beta = (kT)^{-1}$, $P_2(z)$ is the second-order Legendre polynomial [14], and

$$W_2^{(0)}(\mathbf{u}_1, \mathbf{u}_2) = \frac{e^{-\beta V_2^{\text{eff}}(\mathbf{u}_1, \mathbf{u}_2)}}{\int e^{-\beta V_2^{\text{eff}}(\mathbf{u}_1, \mathbf{u}_2)}\, d\mathbf{u}_1\, d\mathbf{u}_2}. \quad (4)$$

The effective orientational pair potential $V_2^{\text{eff}}(\mathbf{u}_1, \mathbf{u}_2)$ is given by

$$V_2^{\text{eff}}(\mathbf{u}_1, \mathbf{u}_2) = U_m^{\infty}(\mathbf{u}_1, \mathbf{u}_2) + U_{an}(\mathbf{u}_1) + U_{an}(\mathbf{u}_2), \quad (5)$$

and $U_{an}(\mathbf{u})$ is obtained from the partial differential equation

$$\nabla_{\mathbf{u}_1} U_{an}(\mathbf{u}_1) = \pm \nabla_{\mathbf{u}_1} U_m^{\infty}(\mathbf{u}_1, \mathbf{u}_3)\big|_{\mathbf{u}_3 = \mathbf{u}_1}. \quad (6)$$

The $\pm$ sign in this last equation reflects the lack of knowledge we have regarding the effect of the third body on the two others and is in fact due to three-body orientational correlation modeling. The mean interaction torque pair potential $U_m^{\infty}(\mathbf{u}_1, \mathbf{u}_2)$ is related to the true pair interaction potential $U_{\text{int}}(\mathbf{r}, \mathbf{u}_1, \mathbf{u}_2)$ by

$$U_m^{\infty}(\mathbf{u}_1, \mathbf{u}_2) = \int_{\frac{2}{\rho_0}} U_{\text{int}}(\mathbf{r}, \mathbf{u}_1, \mathbf{u}_2) G_{\infty}(\mathbf{r})\, d\mathbf{r}, \quad (7)$$

where ρ_0 is the number density so that $2/\rho_0$ denotes the minimal volume of the cavity inside an infinite dielectric in which the molecules are enclosed [13], $G_{\infty}(\mathbf{r})$ is the equilibrium probability density that two molecules are separated by vector $\mathbf{r}$, *viz.*,

$$G_{\infty}(\mathbf{r}) = \frac{e^{-\beta \bar{U}_{\text{int}}^{\infty}(\mathbf{r})}}{\int_{\frac{2}{\rho_0}} e^{-\beta \bar{U}_{\text{int}}^{\infty}(\mathbf{r})}\, d\mathbf{r}} \quad (8)$$

and

$$\bar{U}_{\text{int}}^{\infty}(\mathbf{r}) = \int U_{\text{int}}(\mathbf{r}, \mathbf{u}_1, \mathbf{u}_2) W_2^{(0)}(\mathbf{u}_1, \mathbf{u}_2)\, d\mathbf{u}_1\, d\mathbf{u}_2. \quad (9)$$

The range of validity of Eq. (3) has been qualitatively discussed in Ref. [13]. As is apparent, Eqs. (3)–(9) cannot be self-consistently computed without specifying an initializing potential $U_m^{\infty}(\mathbf{u}_1, \mathbf{u}_2)$ which leads to a specific $V_2^{\text{eff}}(\mathbf{u}_1, \mathbf{u}_2)$, which in turn allows one to calculate $W_2^{(0)}(\mathbf{u}_1, \mathbf{u}_2)$, then to compute Eqs. (8) and (9). More precisely, the true pair intermolecular potential consists of a superposition of a spherically symmetric potential (such as the Lennard-Jones potential) $U_{SR}(r)$ which is strongly repulsive at short intermolecular separations r and which is the dominating part of the interactions in this range, and a long range interaction potential $U_{LR}(\mathbf{r}, \mathbf{u}_1, \mathbf{u}_2)$. This long-range potential depends on only dipole orientations, but also on the pair intermolecular distance $r = |\mathbf{r}|$ *and* $\mathbf{r}$ *orientations* $\hat{r}$, and dominates the intermolecular interactions at large separations r. We generally have

$$U_{\text{int}}(\mathbf{r}, \mathbf{u}_1, \mathbf{u}_2) = U_{SR}(r) + U_{LR}(\mathbf{r}, \mathbf{u}_1, \mathbf{u}_2), \quad (10)$$

which allows the integrals involved in Eqs. (7) and (8) to converge since they are taken over a finite region of space [13], the singularity at $r = 0$ being wiped out by the factor $\exp[-\beta U_{SR}(r)]$, which decreases to zero as $e^{-ar^{-12}}$, $a > 0$ as r approaches zero. Explicitly, we have

$$\bar{U}_{\text{int}}^{\infty}(\mathbf{r}) = U_{SR}(r) + \bar{U}_{LR}^{\infty}(\mathbf{r}), \quad (11)$$

$$\bar{U}_{LR}^{\infty}(\mathbf{r}) = \int U_{LR}(\mathbf{r}, \mathbf{u}_1, \mathbf{u}_2) W_2^{(0)}(\mathbf{u}_1, \mathbf{u}_2)\, d\mathbf{u}_1\, d\mathbf{u}_2, \quad (12)$$

$$U_m^{\infty}(\mathbf{u}_1, \mathbf{u}_2) = C + \int_{\frac{2}{\rho_0}} U_{LR}(\mathbf{r}, \mathbf{u}_1, \mathbf{u}_2) G_{\infty}(\mathbf{r})\, d\mathbf{r}, \quad (13)$$

$$C = \int_{\frac{2}{\rho_0}} U_{SR}(r) G_{\infty}(\mathbf{r})\, d\mathbf{r}, \quad (14)$$

where C is a *finite* constant, and where all integrals *converge*.

B. Application of Eq. (3)

Without being explicit, it is evident that $U_m^{\infty}(\mathbf{u}_1, \mathbf{u}_2)$ consists of an expansion of products of spherical harmonics $Y_{LM}(\mathbf{u}_1) Y_{JK}(\mathbf{u}_2)$ [15]. The values of L, M, J, K are such that $Y_{LM}(\mathbf{u}_1) Y_{JK}(\mathbf{u}_2) = Y_{LM}(-\mathbf{u}_1) Y_{JK}(-\mathbf{u}_2)$ so that U_m^{∞} is globally rotational invariant, i.e., we must have $U_m^{\infty}(\mathbf{u}_1, \mathbf{u}_2) = U_m^{\infty}(-\mathbf{u}_1, -\mathbf{u}_2)$. It is demonstrated in the Appendix that if U_{LR} is the pure dipole-dipole interaction, then ignoring the irrelevant constant C we have the two possibilities for U_m, *viz.*,

$$U_m^{\infty}(\mathbf{u}_1, \mathbf{u}_2) = \mp \frac{\rho_0 \mu^2}{3\varepsilon_0} \cos\vartheta_1 \cos\vartheta_2, \quad (15)$$

where the $-$ sign is for preferred parallel alignment of dipolar pairs, and the $+$ sign holds for preferred antiparallel alignment of dipole pairs and where ϑ_i is the colatitude angle of dipole i. Using $z_i = \cos\vartheta_i$, U_{an} is determined by solving the differential equation

$$\frac{dU_{an}}{dz_1}(z_1) = \pm \left(\frac{\partial U_m^{\infty}}{\partial z_1}(z_1, z_3) \right)_{z_3 = z_1}. \quad (16)$$

Using Eq. (16) to compute U_{an}, we obtain four expressions for $V_2^{\rm eff}$, two of which exhibit a minimum at $(\vartheta_1, \vartheta_2) = (\pi/2, \pi/2)$ and therefore must be discarded, so that the only possibility for $U_{an}(\mathbf{u})$ is, for pure dipole-dipole interactions [16],

$$U_{an}(\vartheta) = -\frac{\rho_0 \mu^2}{6\varepsilon_0} \cos^2 \vartheta. \tag{17}$$

Using Eqs. (25), (15), and (17), this leads to the two possibilities for $V_2^{\rm eff}$,

$$\beta V_2^{\rm eff}(\vartheta_1, \vartheta_2) = -\frac{\lambda}{2}(\cos\vartheta_1 \pm \cos\vartheta_2)^2, \tag{18}$$

where the dimensionless parameter λ is given by

$$\lambda = \frac{\beta \rho_0 \mu^2}{3\varepsilon_0} \tag{19}$$

and measures the ratio of dipole-dipole energy to thermal energy (it is also the dielectric susceptibility of an ideal gas made of polar molecules each carrying a dipole μ). In Eq. (19) μ is given by [2]

$$\mu = \frac{\varepsilon_\infty + 2}{3}\mu_g. \tag{20}$$

Therefore, since all quantities determining λ are known, it follows that this parameter is not adjustable, but known from the measured or *ab initio* calculated characteristics of the liquid and of the molecule itself. In Ref. [17] it was shown that the asymptotic values of $g_{\rm K}$ rendered by Eq. (3) at large λ are 3.5 for preferred parallel alignment and 0.5 for preferred antiparallel alignment, so making the available values of $g_{\rm K}$ at large densities quite restrictive ones, and strictly speaking, hold when the induced dipole moment is ignored. If now one accounts for the polarizability of the molecules, then two extra terms must be taken into account, namely induction and dispersion interactions [18]. We loosely represent these terms as follows:

$$\beta V_{\rm indisp}(\vartheta_1, \vartheta_2) = \mp\kappa\lambda \cos^2\vartheta_1 \cos^2\vartheta_2, \tag{21}$$

where $|\kappa|$ measures the induction or dispersion to dipole-dipole interaction ratio. From now on U_m is given by

$$\beta U_m^\infty(\vartheta_1, \vartheta_2) = \mp\lambda \cos\vartheta_1 \cos\vartheta_2 + \beta V_{\rm indisp}(\vartheta_1, \vartheta_2), \tag{22}$$

where all combination of $\pm$ signs are possible. This gives rise to 16 possible expressions for $V_2^{\rm eff}$, four of which have their stationary points coinciding exactly or approximately with those of U_m given by Eq. (22). Therefore, this in effect gives rise to four possibilities for the Kirkwood correlation factor. These possibilities are summarized in Table I, where in this table and throughout this work the superscript $^{(+)}$ means preferred antiparallel alignment and $^{(-)}$ preferred parallel alignment of dipole pairs. Then, since the interaction potentials have no azimuthal dependence, we can write a simple equation for $g_{\rm K}$, which is

$$g_{\rm K} = 1 - \beta \int_{-1}^{1}\int_{-1}^{1} (1 - z_1^2)\left(z_1 + \frac{3}{2}z_2\right)\frac{\partial U_m^\infty}{\partial z_1}(z_1, z_2) W_2^{(0)}(z_1, z_2)\, dz_1\, dz_2, \tag{23}$$

where

$$W_2^{(0)}(z_1, z_2) = \frac{e^{-\beta V_2^{\rm eff}(z_1, z_2)}}{\int_{-1}^{1}\int_{-1}^{1} e^{-\beta V_2^{\rm eff}(z_1, z_2)}\, dz_1\, dz_2}, \tag{24}$$

and the effective orientational pair potential $V_2^{\rm eff}(z_1, z_2)$ is given by

$$V_2^{\rm eff}(z_1, z_2) = U_m^\infty(z_1, z_2) + U_{an}(z_1) + U_{an}(z_2). \tag{25}$$

$U_{an}(\mathbf{u})$ is a one-body potential loosely accounting for correcting $U_m^\infty(\mathbf{u}_1, \mathbf{u}_2)$ as a result of three-body *orientational* correlations obeying the differential Eq. (16).

III. NUMERICAL RESULTS

Thus, we essentially have four interaction energies U_m^∞, and four corresponding Kirkwood potentials of mean torques $V_2^{\rm eff}$ given in Table I. This leads to four values $g_{\rm K}^{1(-)}$, $g_{\rm K}^{2(-)}$, $g_{\rm K}^{1(+)}$, and $g_{\rm K}^{2(+)}$ that reduce to previously derived results for $g_{\rm K}$ when $\kappa = 0$ [17], i.e., when $V_{\rm indisp}$ is neglected. The variation of $g_{\rm K}^{1(-)}$ as a function of λ and κ is represented in Figs. 1 and 2. One notices the substantial increase of the Kirkwood correlation factor as κ is increased from 0. The explanation is that in this situation, the induction term affects neither the location of the minima (0,0) and (π, π) nor the location of the saddle point of both U_m and $V_2^{\rm eff}$, but *increases* the energy barrier separating the two multidimensional minima in $V_2^{\rm eff}$, which in turn governs the pair equilibrium statistics. As a result, the parallel states (0,0) and (π, π) are made even more (respectively less) probable for $\kappa > 0$ (respectively $\kappa < 0$) than for $\kappa = 0$. This results in an increase (respectively a decrease) in the Kirkwood correlation factor with respect to the situation where $\kappa = 0$. As illustrated in Fig. 2, the variation of $g_{\rm K}^{1(-)}$ with κ for given λ is linear. This means that in this situation, the dipolar field has a trend to induce a dipole in the same direction as that of the alignment of the molecular permanent dipole moments. Thus, the bonds are slightly stretched, so the atomic charge distributions are more distant than in the absence of induced dipoles. The result is

TABLE I. Notations for the Kirkwood correlation factors, interaction potential U_m^∞ and potential of mean torques $V_2^{\rm eff}$. The shorthand notations $z = \cos\vartheta$ and $z' = \cos\vartheta'$ have been used.

	βU_m^∞	$\beta V_2^{\rm eff}$
$g_{\rm K}^{1(-)}$	$-\lambda z z' - \kappa\lambda z^2 z'^2$	$-\frac{\lambda}{2}(z+z')^2 + \frac{\kappa\lambda}{2}(z^2 - z'^2)^2$
$g_{\rm K}^{2(-)}$	$-\lambda z z' + \kappa\lambda z^2 z'^2$	$-\frac{\lambda}{2}(z+z')^2 + \frac{\kappa\lambda}{2}(z^2 + z'^2)^2$
$g_{\rm K}^{1(+)}$	$\lambda z z' + \kappa\lambda z^2 z'^2$	$-\frac{\lambda}{2}(z-z')^2 - \frac{\kappa\lambda}{2}(z^2 - z'^2)^2$
$g_{\rm K}^{2(+)}$	$\lambda z z' - \kappa\lambda z^2 z'^2$	$-\frac{\lambda}{2}(z-z')^2 - \frac{\kappa\lambda}{2}(z^2 + z'^2)^2$

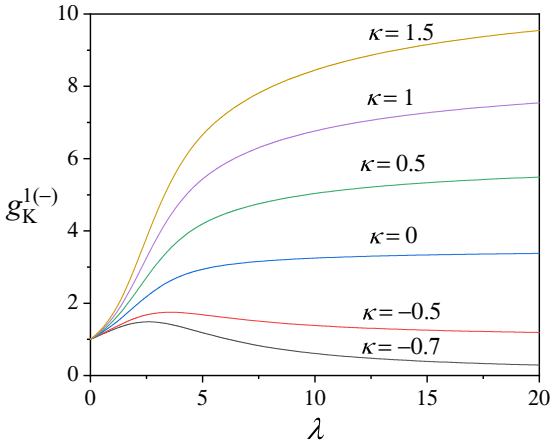

FIG. 1. Kirkwood correlation factor $g_K^{1(-)}$ as a function of λ for various values of κ.

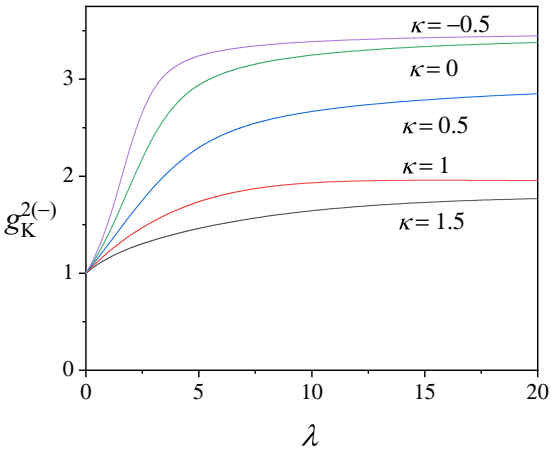

FIG. 3. Kirkwood correlation factor $g_K^{2(-)}$ as a function of λ for various values of κ.

simply a proportion of g_K with κ. We also note from Figs. 1 and 2 that values of $g_K < 1$ are possible *in spite of preferred parallel alignment of the permanent dipoles*. Now, if too large negative κ values are used here, this causes $g_K^{1(-)}$ to take unphysical negative or null values. The higher transcendental nature of the functions representing the integrals makes it difficult to precisely state the limiting κ value at which this occurs, nevertheless these integrals can straightforwardly be computed numerically. Therefore, if any negative κ value is to be applied when comparing the present theory with experiments, then one must guarantee the positiveness of $g_K^{1(-)}$ in the whole temperature range where the species under study is in its liquid phase.

Figures 3 and 4 show the behavior of $g_K^{2(-)}$ when λ and κ are varied. In this situation, the locations of the minima of V_2^{eff} are affected in raising κ, while the saddle point remains unchanged. Thus, the strictly parallel equilibrium states are affected, and pairs of dipoles form an angle at equilibrium, so that the pair alignment state is *a canted one*. The energy barrier separating the two minima is furthermore lowered, and therefore the equilibrium states are less populated with respect to the situation where $\kappa = 0$. Altogether, this results in a decrease of g_K. Unlike for $g_K^{1(-)}$, the behavior of $g_K^{2(-)}$ with κ is not linear at all. Here a tentative explanation may be that the term V_{indisp} fights nontrivially against the aligning effect of the permanent dipole moments due to V_{dd}. Altogether, the equilibrium parallel alignment of permanent dipoles is affected. The angle between a pair of dipoles in the wells is not so well defined in this situation, as our simplified interaction potentials are azimuth-independent, so that in the present model transverse modes are energy costless modes. Nevertheless, according to our model, we may state that the relative orientation of dipole pairs at equilibrium obeys the double inequality:

$$0 \leqslant \vartheta_{(\mathbf{u},\mathbf{u}')} \leqslant 2 \arctan \frac{\sqrt{\sqrt{1+16\kappa^2}-1}}{\sqrt{2}}, \tag{26}$$

where the upper bound is equal to $\Theta = \vartheta_{\min} + \vartheta'_{\min} = 2\vartheta_{\min}$ and $(\vartheta_{\min}, \vartheta'_{\min})$ is the location of one of the deepest symmetric minima of the corresponding Kirkwood potential of mean torques V_2^{eff}, while the lower bound is given by $\vartheta_{\min} - \vartheta'_{\min} = 0$. Thus, the relative orientation of dipole pairs may be *larger* than $\pi/2$, in spite of the fact that in this situation, $g_K > 1$. In order to illustrate this, we have plotted the quantity Θ as a

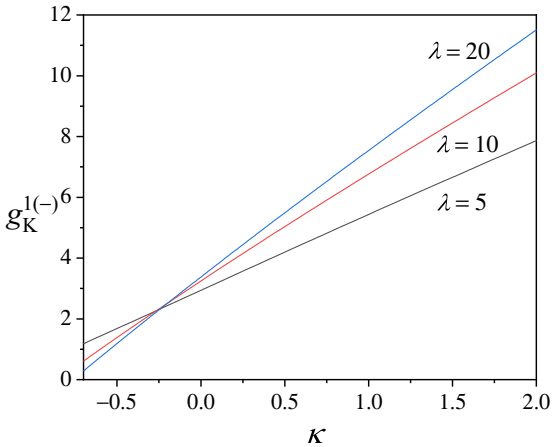

FIG. 2. Kirkwood correlation factor $g_K^{1(-)}$ as a function of κ for various values of λ.

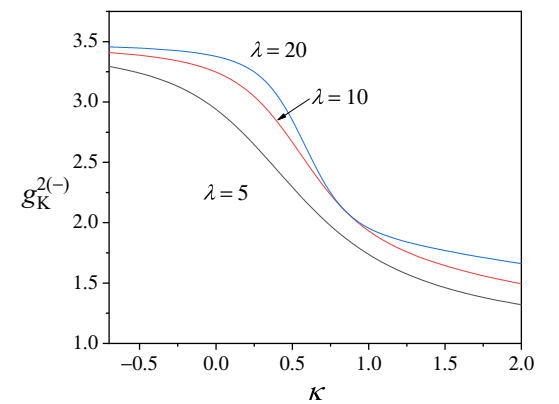

FIG. 4. Kirkwood correlation factor $g_K^{2(-)}$ as a function of κ for various values of λ.

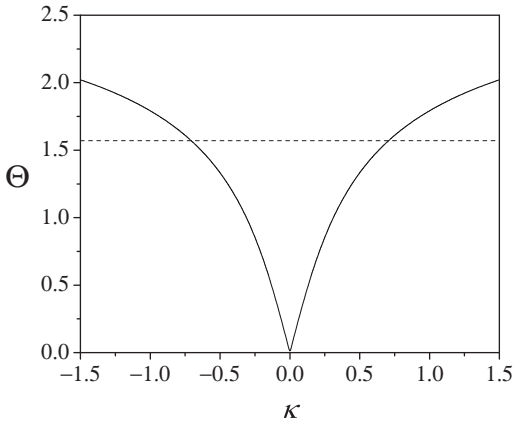

FIG. 5. The maximal relative orientation of dipole pairs Θ as a function of κ. The dashed line is the $\pi/2$ relative orientation.

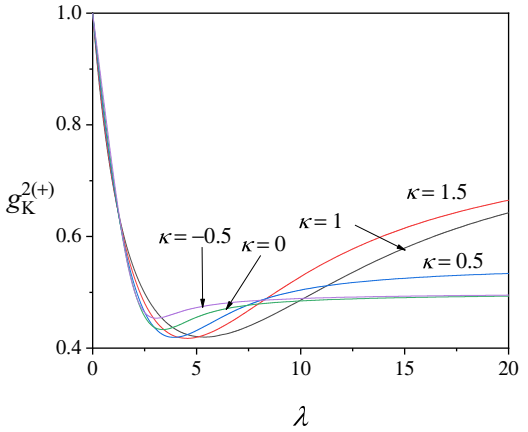

FIG. 7. Kirkwood correlation factor $g_K^{2(+)}$ as a function of λ for various values of κ.

function of κ in Fig. 5, where it becomes clear that Θ may be larger than $\pi/2$ at some κ values.

Thus, in particular, $g_K > 1$ *does not guarantee the parallel alignment of dipole pairs at equilibrium*. In the next section we give a comparison of our calculations with the experimental temperature dependence of the static linear permittivity of tributyl phosphate in order to illustrate the situation we just described. The variation of $g_K^{1(+)}$ and $g_K^{2(+)}$ with λ for various values of κ are shown in Figs. 6 and 7. These values of the Kirkwood correlation factor correspond to preferred antiparallel alignment when $\kappa = 0$. The most remarkable feature of $g_K^{1(+)}$ is that in this situation, the Kirkwood correlation factor is able to exhibit both g_K values that are smaller and larger than 1, and that this happens at moderate values of λ. Furthermore, for $\kappa > 0$, $g_K^{1(+)}$ is able to render negative values of g_K if $|\kappa|$ takes too large values, so that the same prescriptions as those given above for $g_K^{1(-)}$ apply to $g_K^{1(+)}$ when attempting a comparison with experimental data.

The variation of $g_K^{1(+)}$ and $g_K^{2(+)}$ with κ is shown in Figs. 8 and 9. As for $g_K^{1(-)}$, the variation of $g_K^{1(+)}$ with κ is linear, so that the stretching of molecular bonds has the same effect as that for $g_K^{1(-)}$. In fact, here the extra dipole is induced in the direction opposite to the permanent dipole alignment direction, leading to an overall increase of g_K, therefore to an increase of the dielectric constant with respect to the situation where $\kappa = 0$. At last, in this situation, the minima of the potential V_2^{eff} are those of antiparallel alignment.

In contrast, the variation of $g_K^{2(+)}$ with κ is not linear at all. Here the explanation is different from the κ behavior of variation of $g_K^{2(-)}$. In effect, for positive κ, the Kirkwood potential of mean torques V_2^{eff} exhibits two pairs of unequal minima in a cycle of the motion of dipole pairs, located both at the parallel and antiparallel states. This altogether affects the g_K value in a nontrivial way, depending on the λ values. For negative κ, the equilibrium orientations of the permanent moments are spread over the range:

$$\pi - 2\arctan\frac{\sqrt{\sqrt{1+16\kappa^2}-1}}{\sqrt{2}} \leqslant \vartheta_{(\mathbf{u}_1,\mathbf{u}_2)} \leqslant \pi\,. \qquad (27)$$

This is similar to the behavior of $g_K^{2(-)}$ as in this situation, dipoles are induced in such a way that they are parallel. Here g_K is near 0.5, as if the induction term did not significantly affect orientational correlations.

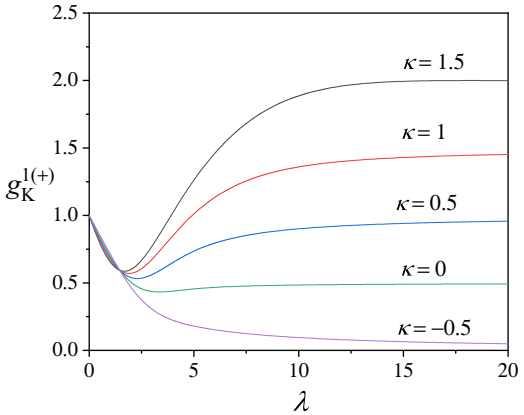

FIG. 6. Kirkwood correlation factor $g_K^{1(+)}$ as a function of λ for various values of κ.

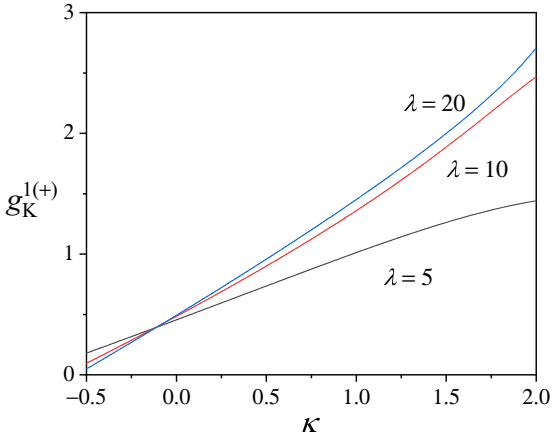

FIG. 8. Kirkwood correlation factor $g_K^{1(+)}$ as a function of κ for various values of λ.

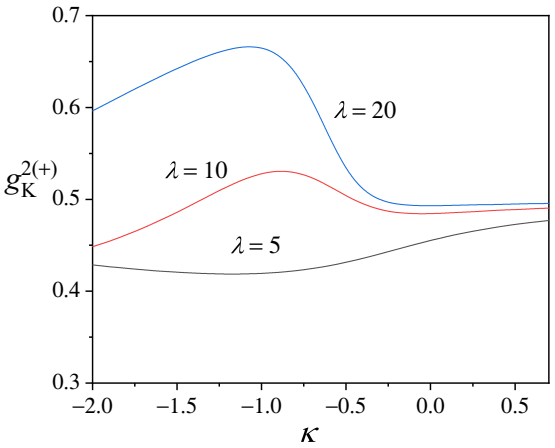

FIG. 9. Kirkwood correlation factor $g_K^{2(+)}$ as a function of κ for various values of λ.

IV. COMPARISON WITH EXPERIMENTAL DATA

In this section we compare our theoretical findings with experimental data. In order to do so, we use static dielectric permittivity values either from the literature, i.e., unless stated otherwise, values from Wohlfarth's Landolt-Bornstein tables [19] or from our own measurements, and compare them to calculated values employing the theory described in the foregoing sections. In the Kirkwood-Fröhlich theory, the dielectric constant is given by

$$\varepsilon = \tfrac{1}{4}\left[3\lambda g_K + \varepsilon_\infty + \sqrt{8\varepsilon_\infty^2 + (3\lambda g_K + \varepsilon_\infty)^2}\right], \tag{28}$$

where

$$\lambda = \lambda(T) = \frac{M_v(T) N_A \mu_g^2 [\varepsilon_\infty(T) + 2]^2}{27 M_{\mathrm{mol}} \varepsilon_0 kT}. \tag{29}$$

Here the experimentally measured temperature-dependent mass density of the polar fluid $M_v(T)$ is sometimes extrapolated to the temperature of interest either via the equations given in the respective references or via a linear law fitted to the measured values when this expression is valid in the whole range of temperatures considered. Furthermore, in Eq. (29), following Onsager *et al.* [4–6], we set

$$\varepsilon_\infty = \varepsilon_\infty(T) = n^2(T), \tag{30}$$

where n is the mean refractive index of the fluid measured for the sodium D spectral line (also sometimes extrapolated to the temperature of interest either via the equations given in the respective references or via a linear law fitted to the measured values). For some polar fluids we compute n from the Lorenz-Lorentz equation,

$$\frac{n^2(T) - 1}{n^2(T) + 2} = \frac{M_v(T) N_A \bar{\alpha}}{3 M_{\mathrm{mol}} \varepsilon_0}, \tag{31}$$

where $\bar{\alpha}$ is the mean molecular polarizability, taken from the literature.

The Kirkwood correlation factor g_K in Eq. (28) is, according to our theory, dependent on $\lambda(T)$ and κ, and four different functions for $g_K(\lambda(T), \kappa)$ are possible according to Table I. By substituting the respective U_m and V_2^{eff} into Eq. (3), the Kirkwood correlation factor is calculated by numerical integration because the exact numerical value of the integral is required for comparing the outcomes of the theory with experiment.

As mentioned above, κ can be regarded as a measure of the strength of the induction- or dispersion-type interaction and is the only unknown parameter which is needed to calculate the theoretical Kirkwood correlation factor. It is expected that κ is somehow related to the molecular polarizability $\bar{\alpha}$ and/or the asymmetry of the molecular polarizability tensor; however, in the current state of our theory, it can not be determined explicitly, and thus it is left as the only fitting parameter to achieve agreement between theory and experiment. The choice between the four different representations of $g_K(\lambda(T), \kappa)$ is based upon some possibly existing foreknowledge about the preferred alignment from the literature and/or based upon the comparison of the theoretical and experimental temperature dependences of the static permittivity. Since the four $g_K(\lambda, \kappa)$ have distinct slopes depending on $\lambda(T)$, as can be seen in Figs. 1, 4, 6, and 7, *this results in an unambiguous assignment of one* $g_K(\lambda, \kappa)$ to the respective polar fluid.

In the following subsections we discuss the comparison of theory and experiment for different classes of polar liquids. An overview of all substances under study, including all values needed to calculate the Kirkwood correlation factor, is given in Table II.

A. Parallel alignment: Linear primary alcohols

We start with a series of linear primary alcohols with different alkyl-chain length, for which preferred parallel alignment of the dipole moments, which are located at the O-H group at one end of the carbon chain, is well known. Different values for this dipole moment of linear primary alcohols are found in the literature, and these values usually range between 1.65 and 1.70 D [21]. Since the total dipole of a molecule is the sum of the dipole moments of its chemical bonds, and the C-H bonds are almost apolar, the permanent dipole moment of all linear primary alcohols should be the same in a first approximation. An average value of 1.68 D thus has been chosen as the value of μ_g for all the considered linear primary alcohols.

In Fig. 10 the experimental static permittivities for all alkyl-chain lengths from methanol to octan-1-ol are shown as plain circles, together with the theoretical values calculated using $g_K^{1(-)}$ as solid lines.

As one can see, the agreement of the theoretical with the experimental values is excellent for all linear primary alcohols over the whole temperature range where experimental data are available. The values of κ, which are chosen in order to achieve this agreement, are shown in the inset of Fig. 10. It is obvious that κ increases with increasing number of carbon atoms in the alkyl chain, which indicates the increasing strength of the induction- or dispersion-type interaction. Since the polarizability of a molecule increases with its molecular mass while the permanent dipole moment is the same for all molecules of this series, this finding is perfectly reasonable and underlines the importance of the induction- or dispersion-type interaction for larger molecules, which we hope to treat more consistently than here in future work. However, it is clear that the κ parameter does not depend linearly on the number of carbon atoms in the alkyl chain, which shows that the latter parameter is not a trivial function of the polarizability, particularly as a result of nonadditivity

TABLE II. Parameters used in the computation of the static permittivity (28). Mean molecular polarizabilities from Ref. [20]. Molecular dipole moments from Ref. [21] except (*a*) from Ref. [22] and (*b*) from Ref. [23], which is the value of the dipole moment of TBP in decalin, which is a nonpolar solvent that has no influence on the molecular TBP dipole. (*c*) We performed refractive index measurements between 10 °C and 50 °C using an Abbe refractometer.

	μ_g (D)	$\bar{\alpha}$ (Å^3)	κ	g_K	$M_v(T)$	$n(T)$
Methanol	1.68	–	0.04	$g_K^{1(-)}$	Ref. [24]	Ref. [25]
Ethanol	1.68	–	0.05	$g_K^{1(-)}$	Ref. [24]	Ref. [25]
Propan-1-ol	1.68	–	0.22	$g_K^{1(-)}$	Ref. [26]	Ref. [25]
Butan-1-ol	1.68	–	0.35	$g_K^{1(-)}$	Ref. [24]	Ref. [25]
Pentan-1-ol	1.68	–	0.5	$g_K^{1(-)}$	Ref. [27]	Ref. [25]
Hexan-1-ol	1.68	–	0.65	$g_K^{1(-)}$	Ref. [28]	Ref. [25]
Heptan-1-ol	1.68	–	1.05	$g_K^{1(-)}$	Ref. [29]	Ref. [25]
Octan-1-ol	1.68	–	1.5	$g_K^{1(-)}$	Ref. [30]	Ref. [25]
Water	1.845	1.501	−0.15	$g_K^{1(-)}$	Ref. [24]	L.-L.
Acetonitrile	3.92	4.44	0.345	$g_K^{1(+)}$	Ref. [24]	L.-L.
Nitrobenzene	4.02[a]	12.26	0.67	$g_K^{1(+)}$	Ref. [31]	L.-L.
Acetone	2.88	6.27	0.83	$g_K^{1(+)}$	Ref. [24]	L.-L.
DMSO	3.96	7.97	0.73	$g_K^{1(+)}$	Ref. [32]	Ref. [32]
TBP	2.6[b]	–	0.85	$g_K^{2(-)}$	Ref. [33]	Own[c]
Glycerol	2.67	7.80	−0.3	$g_K^{1(-)}$	Ref. [34]	L.-L.

of induction-dispersion energies [18]. Therefore, the determination of κ from molecular properties is beyond the scope of this work and thus is left as a fitting parameter.

As indicated by the use of $g_K^{1(-)}$, the preferred dipolar order in these substances is, as is well known, the parallel one. The temperature dependence of the calculated Kirkwood correlation factor is shown in Fig. 11, only for some of these substances for clarity.

It is obvious that the slope of $g_K(T)$ is nontrivial and behaves distinctly different for various linear alcohols and it agrees with those found experimentally in the literature [2]. Therefore, by adjusting the strength of the induction- or dispersion-type interaction via the temperature-independent κ, our theory is able to calculate the correct Kirkwood correlation factor and thus reproduces the experimental static permittivities using the correct dipole moment in the gas phase μ_g. Last, since the graphical representation of $g_K^{1(-)}(\kappa)$ is a straight line, there is a bijective correspondence between a selected value of κ and ε, so that our theoretical uncertainty on all calculated parameters *is zero*.

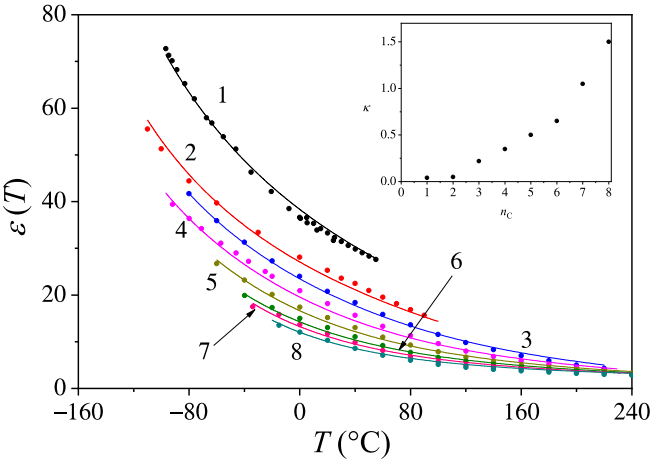

FIG. 10. Experimental temperature dependence of the linear static permittivity of methanol (1), ethanol (2), propan-1-ol (3), butan-1-ol (4), pentan-1-ol (5), hexan-1-ol (6), heptan-1-ol (7), and octan-1-ol (8). Solid line: theory. Dots: experimental data from Ref. [19]. For heptan-1-ol, the experimental data are the same as those published by Vij *et al.* [35] at normal pressures. Inset: variation of κ with the number of carbon atoms n_C in the alkyl chain.

B. Antiparallel alignment

In this subsection, we compare our theory with experimental static permittivities of substances, for which it is known from techniques other than dielectric spectroscopy, that they

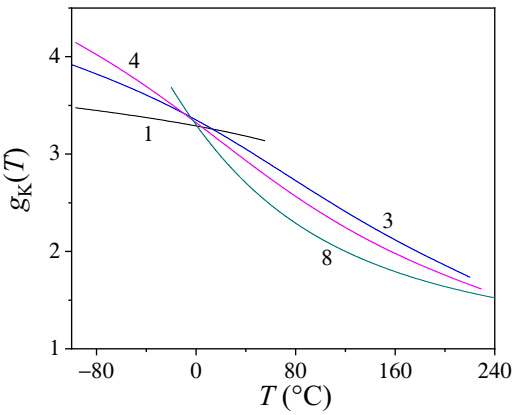

FIG. 11. Experimental temperature dependence of the Kirkwood correlation factor of methanol (1), 1-propanol (3), 1-butanol (4), and 1-octanol (8).

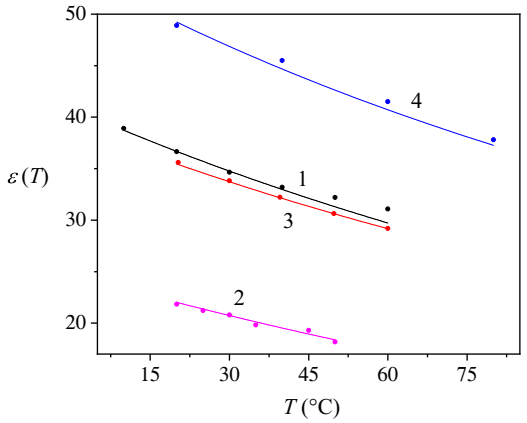

FIG. 12. Experimental temperature dependence of the linear static permittivity of acetonitrile (1), acetone (2), nitrobenzene (3), and DMSO (4). Solid line: theory. Dots: experimental points [19]. DMSO data, including density and refractive index from Schläfer *et al.* [32].

exhibit preferred antiparallel dipolar ordering. These substances are acetonitrile [36], nitrobenzene [37], acetone [38], and dimethyl sulfoxide (DMSO) [38]. Comparison between theory and experiment is shown in Fig. 12. Experimental data for these substances are available only over a narrow temperature range. However, as can be seen in Fig. 13, the Kirkwood correlation factors hardly depends on temperature, thus this is not too much a drawback.

1. Acetonitrile and acetone

Our theoretical estimates of the static permittivity of acetonitrile (ACN) apparently deviate from the experimental data of Stoppa *et al.* [39] at high temperatures, of at most 4.7%, while yielding good agreement at the lowest ones. It is difficult to believe that the deviation between theory and experiment is due to a poor representation of intermolecular interactions as λ takes rather low values at high temperatures. Yet our theoretical findings remains not too far from the experimental data. For ACN, the Kirkwood correlation factor remains almost

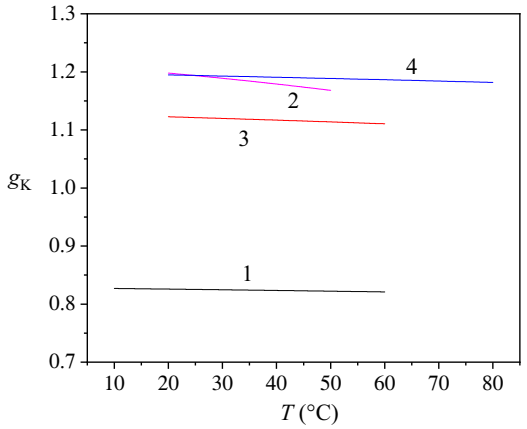

FIG. 13. Theoretical temperature dependence of Kirkwood correlation factor of acetonitrile (1), acetone (2), nitrobenzene (3), and DMSO (4).

temperature independent between 10 °C and 60 °C, yielding $g_K \approx 0.82$. Since $g_K^{1(+)}$ is used, the dipolar order is strictly antiparallel, as expected. These values agree reasonably well with the experimentally deduced values of Helambe *et al.* [40] in the pure liquid phase.

Our theoretical estimates of the static permittivity of acetone are in good agreement with the experimental ones. We also find antiparallel order for acetone, using $g_K^{1(+)}$ as a representative of g_K. This substance exhibits the strongest temperature dependence of g_K out of the four substances discussed in this subsection, as illustrated in Fig. 13. Our values decrease from 1.22 to 1.19 when the temperature is increased from 20 °C to 50 °C, and are slightly above the value at 25 °C of pure acetone by Kumbharkhane *et al.* [41] which is 1.02, while Vij *et al.* [42] found the value 1.38. Our values are framed between both experimentally determined ones, and therefore, our theoretical findings may be considered as satisfactory for this substance in the considered temperature range. We emphasize that due to the relatively large value of $\kappa = 0.83$, the g_K values of acetone are above unity, *despite preferred antiparallel alignment*.

2. Nitrobenzene and DMSO

The same is true for Nnitrobenzene and DMSO, where a Kirkwood correlation factor larger than unity (see Fig. 13) reproduces the experimental data in Fig. 12 quite well, employing $g_K^{1(+)}$, i.e., antiparallel alignment.

We emphasize here again that the expectation that antiparallel dipolar alignment has to result in a Kirkwood correlation factor of less than unity has led, for example, Shikata *et al.* [43], like many authors (including two of us [44] for methanol, for example), to use too high of a value of $\varepsilon_\infty = 3.5$ by treating ε_∞ as a fitting parameter, in order to obtain $g_K = 0.65 < 1$ for nitrobenzene. Again this procedure is misleading and results in some cases in somewhat arbitrary choices of ε_∞, just to fulfill the expectations about the value of the Kirkwood factor in comparison with unity.

We also note here that great care must be taken regarding the frequency at which the dielectric constant is measured. If measurements are performed at a fixed frequency instead of measuring a spectrum over several orders of magnitude in frequency, one has to be sure that this frequency is sufficiently low to neglect relaxation effects but also sufficiently high so that one also can neglect electrode polarization effects stemming from ionic impurities, which might be present in some occasions. This is actually one of the reasons why it is very difficult to determine the dielectric constant of supercooled liquids as the glass temperature transition is approached from above.

For example, in the case of DMSO we have compared our theoretical findings with the data of Schläfer *et al.* [32], who report measurements of the static permittivity at a measuring frequency of 100 kHz. We were quite surprised that the data of Schläfer *et al.* were the only ones (see Ref. [19]) that we were able to interpret. Yet they are the sole data of Ref. [19] which, in our opinion, truly reflect the static permittivity of DMSO, because all data but those of Schläfer *et al.* were recorded at least at a ten times higher frequency, indicating that dipolar relaxation might play a role, so that the

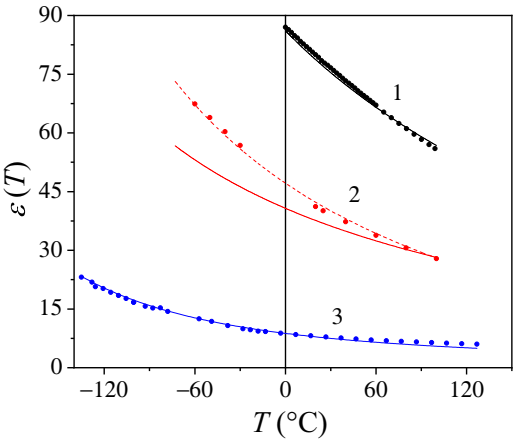

FIG. 14. Experimental temperature dependence of the linear static permittivity of water (1), glycerol (2), and TBP (3). Solid line: theory. Dots: experimental points. Dashed line: empirical equation of Matyushov and Richert [47] for glycerol.

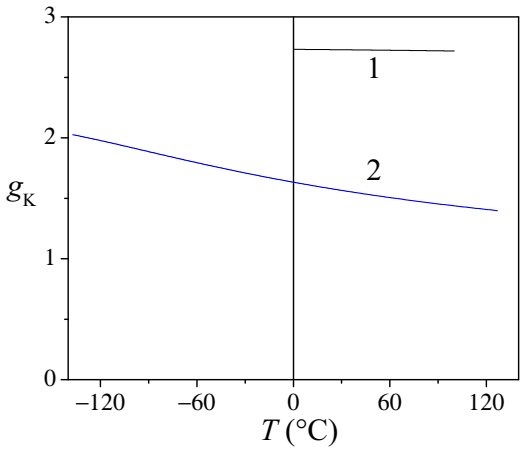

FIG. 15. Theoretical temperature dependence of Kirkwood correlation factor of water (1) and TBP (2).

measured permittivities can no longer be considered as the static ones.

We note in passing that Schläfer *et al.* quote a dipole value of DMSO $\mu_g = 4.3 \pm 0.1$ D, using Onsager's equation [4]. In effect, we find that the Onsager dipole $\mu_g\sqrt{g_K}$ varies between 4.28 and 4.32 D, in agreement with the experimental one and lies in the experimental uncertainty window. Finally, we remark that Onsager's equation [4] is generally most successful in polar substances with antiparallel order (one exception being liquid water) because as illustrated in Fig. 13, generally g_K has almost no temperature dependence. However, as explained by Coffey [45] and later in Ref. [46], this equation is difficult to understand from a microscopic point of view. Yet it is useful because it yields a relatively good estimate of the dipole moment μ_g in dilute situations, for example, using Malecki's method [22].

C. Special cases: Water, TBP, and glycerol

In this subsection we compare our theory to experimental values of three special liquids: water, glycerol, and tributyl phosphate (TBP). The specialties of these substances will become clear in the following. Figure 14 displays the experimental ε values as points and the theoretical ones as solid lines for these three liquids.

1. Water

A comparison of experimental static permittivities of water with an earlier stage of our theory was already given in Ref. [17]. Therein, the induction- or dispersion-type interaction was not yet accounted for, the refractive index was kept temperature independent and $\varepsilon_\infty = 1.03n^2$ was chosen. This leads to a disagreement with the experimental data at temperatures above 80 °C. Here the induction and dispersion effects together with inclusion of the temperature dependence of n allows our theoretical findings to agree with experimental data across the whole temperature range. The κ parameter was adjusted to -0.15 to achieve this agreement, indicating a slight reduction of the total effective dipole moment $(\varepsilon_\infty + 2)\mu_g/3$. Moreover it indicates a specific equilibrium geometry of the water molecules in the liquid phase, which, however, is impossible to specify precisely in the present context.

The Kirkwood correlation factor of liquid water as a function of temperature is shown in Fig. 15. For water, it is known that the experimental Kirkwood correlation factor is $g_K = 2.75$ at 0 °C [2] and decreases to $g_K = 2.49$ at $T = 83$ °C, under the conditions that $\varepsilon_\infty = 1.05n^2$ and ε_∞ is temperature independent [2]. In the present work, we find $g_K = 2.73$ at $T = 0$ °C and $g_K = 2.72$ at $T = 83$ °C, however, under the condition $\varepsilon_\infty(T) = n^2(T)$, with n^2 obeying the Lorenz-Lorentz Eq. (31). Since we use $g_K^{1(-)}$ as a representative of g_K for this substance, the dipolar order in liquid water is the parallel one, in agreement with the Oster-Kirkwood predictions [5,48]. We also remark, that, incidentally, the g_K is basically independent of temperature, which explains why Onsager's equation works at room temperature for liquid water with values of ε_∞ as large as 4.5 [2,49]. Again this exaggerated value of ε_∞ has led many authors, including two of us [17,50], to treat ε_∞ as a fitting parameter, in order to obtain values of g_K that comply with what is believed about dipolar order in water. We insist again that this procedure is misleading and has no serious theoretical grounding at all. Finally we note that our present calculations for g_K of water are also in reasonable agreement with the molecular dynamics (SPC/E) numerical simulations of van der Spoel *et al.* [51]

2. TBP

Tributyl phosphate (TBP) is special in so far as it is the only substance—out of all we tested so far—where $g_K^{2(-)}$ has to be employed to achieve agreement between theory and experiment. The experimental static permittivities, which are shown in Fig. 14, were obtained in our laboratory. Details of the experimental setup are described elsewhere [52]. As can be seen in this figure, the theory is able to describe the experimental data over a temperature range of more than 260 K, and since the glass transition temperature of TBP is about $T_g = -132$ °C [53], we may consider that unlike what was stated in Ref. [17], the theory is *sometimes* able to predict correct values of the static permittivity even below the calorimetric T_g.

The temperature variation of g_K for TBP is shown in Fig. 15. Clearly, for this substance, $g_K > 1$. However, since $g_K^{2(-)}$ is used here with $\kappa = 0.85$, the permanent dipole pair relative orientations continuously spread between 0° and 97°, as obtained from Eq. (26). This means that both parallel and antiparallel alignment of dipolar pairs are present in this substance.

A Kirkwood correlation factor of less than unity was obtained in a different study by Saini *et al.* [53] and thus needs a comment: The value of the molecular dipole moment μ_g of tributyl phosphate (TBP) used in their study is 3.1 D, which is the value of TBP dissolved in carbon tetrachloride. Although this solvent is nonpolar, it still affects the value of μ_g as it has a non-negligible effect on the phosphoryl group [23]. We used the value of 2.60 D, which is obtained in an octane solution and is almost identical to the value obtained in a decalin solution [23], both unpolar solvents without influence on the TBP molecules.

Moreover, in the work of Saini *et al.*, $\varepsilon_\infty \approx 5$ was used, which is far from $\varepsilon_\infty = n^2$. This value was read off the spectrum at frequencies lower than the strong secondary relaxation, which is clearly due to molecular reorientation. Thus, this choice is not justified in our opinion and leads together with the too high dipole moment to a g_K value less than unity.

The value 3.32 D of undiluted TBP quoted by Petkovic *et al.* [23] is the one compatible with Onsager's equation at room temperature. If we use the Onsager dipole $\mu_g\sqrt{g_K}$ with our calculated g_K, we find 3.27 D at room temperature, which is rather close to Petkovic's result.

3. Glycerol

As can be seen in Fig. 14, the experimental data points of glycerol cannot be described by our theory at all. Here we show the calculated values for $g_K^{1(-)}$, however, also no other representation of g_K is able to reproduce the experimental values with physically reasonable values of the parameters.

Often the specificity of H-bonding is invoked in order to explain disagreement between theory and experiment. This is not so here, since H-bonding specific mechanisms are not needed at all in order to obtain agreement between theory and experiment for linear primary alcohols and water, both prominent examples of H-bonding liquids. Rather, we believe that the disagreement is explained by the oversimplification of the interaction potential (22) which, in effect, pertains to molecules having their permanent dipole moment fixed with respect to a given axis of symmetry of the molecule. Thus, due to the floppyness of the glycerol molecules, and due to the fact that comparable contributions to the overall dipole moment are located in different positions in the molecule, the situation for glycerol is quite different. Owing to this reason, we believe that the interaction energy landscape is much too simple to capture the main physics which is necessary for the theoretical description of the temperature dependence of the dielectric constant of this polar fluid. We note that the seemingly good agreement between theory and experiment with the potential (22) can be forced across the whole temperature range using the unphysical assumption $\varepsilon(T) = 0.5n^2(T)$ together with $g_K = g_K^{1(-)}$ and $\kappa = 0.45$. The relation $\varepsilon(T) = 0.5n^2(T)$ used in such a fit actually reveals that the reason of our failure indeed lies in the oversimplification of the intermolecular interaction potential (22) and the resulting Kirkwood potential of mean torques V_2^{eff} rather than in the specific H-bonding mechanism, which is not explicitly accounted for. Therefore, we state that glycerol is a nonsimple polar fluid (and even less a simple liquid), where the intermolecular interaction is not appropriately represented in our theory and thus, the substance is out of scope of the present work.

V. SUMMARY OF RESULTS AND PERSPECTIVES

In this work, we have computed the Kirkwood correlation factor of simple polar fluids from Eq. (3) which was derived in a companion paper [13] and we have successfully compared the outcomes of this formula with experimental data regarding the temperature dependence of the linear dielectric constant of simple polar fluids. This equation has a lot of advantages, the first one being that it is independent on the number of neighbors and that no molecule needs to be tagged to achieve the calculation, the second being the fact that the approach easily lends itself to tractable approximations, and the third one being that our theory is quantitatively amenable to comparison with experiment. We have also suggested how to construct a model potential for the electrostatic interaction that not only includes the permanent electric dipoles but also in the next order some induction- and dispersion-like effects. Finally, for each case of preferred parallel or antiparallel alignment of permanent dipoles and their modification by induced polarization, two different Kirkwood potentials of mean torques are deduced, for which Eq. (3) is calculated numerically to yield respective temperature-dependent values of the static dielectric constant and the Kirkwood correlation factor. The models contain only physical quantities, like density, permanent dipole moment and refractive index, or molecular polarizability, respectively, that are independently accessible by experiment. Only one single material specific and temperature independent parameter enters the calculation, which is connected to the molecular polarizability, which cannot be calculated from the latter in a straightforward manner and thus needs to be a fitting parameter. In that way we are able to quantitatively compare the calculated values of $\varepsilon(T)$ with experimental data, and it turns out that the derived model potentials seem to capture the underlying main physics of different system classes to a rather good accuracy, at least from the point of view of a static dielectric constant measurement.

A first important result from these calculations is the observation that a parallel alignment of the dipole pairs does not necessarily imply $g_K > 1$, and similarly an antiparallel alignment of dipole pairs does not strictly imply $g_K < 1$ either. Rather, such alignment states are local minima of the effective pair interaction orientational potential of mean torques, for which not only permanent but also induced dipole moments play a decisive role. For example, applying Eq. (26) to TBP, we find that pairs of dipoles in this polar substance have a trend to make angles spreading between 0° and 97°, explaining quantitatively the value of $g_K \approx 2$ of TBP near its glass transition temperature and beyond [52].

We also discuss several examples of preferred antiparallel alignment, not only for acetonitrile, where $g_K < 1$ is found as expected, but also for acetone, nitrobenzene and dimethyl

sulfoxide, where despite the antiparallel alignment clearly $g_K > 1$ due to the non-negligible influence of the molecular polarizability. This again underlines that the usual arguments relating parallel ($g_K > 1$) and antiparallel ($g_K < 1$) alignments based on an oversimplified interpretation of Eq. (2) hampers comparison of the results found from linear dielectric measurements concerning dipolar alignment with those obtained from other characterization techniques.

As examples for a preferred parallel alignment of dipoles we have investigated a series of linear monohydroxy alcohols, where our theory reproduces the experimental $\varepsilon(T)$ for the full series from methanol to octanol with the importance of the polarizability component increasing with molecular volume (the number of carbon atoms involved in the alkyl chain), as expected. Moreover, the static permittivity of liquid water from the melting temperature to the boiling point shows excellent agreement with the theory. This is quite remarkable, as the theory does not explicitly contain any particular H-bonding-related mechanism. Thus, the idealization of a molecule which consists of its permanent and induced dipole moments only is enough to explain the temperature dependence of the static dielectric constant of these hydrogen bonding liquids as first Debye, Kirkwood, and Fröhlich assumed [1,2,6]. Interestingly, the situation is different for the polyalcohol glycerol. Here apparently our model for the pair potential is too simple to capture the actual electrostatic interaction. The reason for this is unlikely the specific role of hydrogen bonds, because our theory compares favorably with experimental data concerning water and monoalcohols. More likely, it may be suspected that since the dipole moment of glycerol is composed of the moments located in three different OH groups within the molecule, considerable intramolecular flexibility leads to a rather ill defined molecular dipole moment, resulting in turn in more complicated interactions. Work to develop appropriate interaction potentials for such associated molecular liquids is in progress.

In spite of the fact that our theory covers a large spectrum of values for g_K, it still does not explain the experimental temperature variation of the dielectric constant of some carboxylic acids and also a couple of monohydroxy alcohols, where a minimum in the temperature dependence of the dielectric constant is observed. For example, the dielectric constant of acetic and caprylic acid [2] or of certain octanol isomers [54,55] first decreases with temperature, but then *increases* again. In fact, such unusual behavior of $\varepsilon(T)$ is usually explained by the simultaneous presence of hydrogen-bonded closed-ring structures, for which the net dipole moment is approximately zero, together with linear multimer chains with various concentrations [2]. A minimal modeling of such behavior may require to consider two different species in the sample and correspondingly different λ factors appropriately weighted by the temperature-dependent molar fractions of closed rings and linear chains, respectively. Testing of such ideas is currently in progress.

Certainly more demanding will be to adapt the present theory to binary *polar* mixtures. Here a zero-order approximation for evaluating the static dielectric constant might be to consider the coupled Langevin equations for the overdamped nonlinear itinerant oscillator model [56] with a specific pair interaction potential and the corresponding equilibrium Smoluchowski equation [57] to deduce equilibrium properties. Moreover, one may also try to extend the present model to dynamics, similar to previous work [16], in both linear and nonlinear responses. Finally, one could also think of applying the present calculations to suspensions of magnetic nanoparticles similar to what was already pointed out previously [16,58]. The development of the theory in all of these directions is currently in progress.

In conclusion, the static limit of the kinetic Yvon-Born-Green theory proposed in Ref. [13], is able to *quantitatively* reproduce the temperature behavior of the dielectric constant and Kirkwood correlation factor of simple polar fluids. This theory particularly extends current DDFT approaches to the problem [59,60]. The corresponding dynamics may also be computed, and continuous distributions of relaxation times included in the theory [13], so that this "extended DDFT" or kinetic Yvon-Born-Green approach constitutes a strong corpus for developing the theory of linear and nonlinear dipolar relaxation in condensed phases.

ACKNOWLEDGMENTS

T.B., F.P., and A.H. gratefully acknowledge financial support by the Deutsche Forschungsgemeinschaft under Grant No. BL 1192/3.

APPENDIX: DIPOLE-DIPOLE INTERACTIONS FOR PURELY POLAR MOLECULES

Here we derive the form of U_m^∞ arising from dipole-dipole interactions, where we assume that all densities are normalized to unity. Thus, the dipole-dipole interaction for a pair of identical molecules is

$$U_{\rm int}(\mathbf{r}, \mathbf{u}_1, \mathbf{u}_2) = \frac{\mu^2}{4\pi\varepsilon_0 r^3}\mathbf{u}_1 \cdot \mathbf{T}(\hat{r}) \cdot \mathbf{u}_2, \tag{A1}$$

where $\mathbf{T}(\hat{r})$ is a tensor that can be written in dyadic form as follows:

$$\mathbf{T}(\hat{r}) = \mathbf{I} - 3\hat{r}\hat{r}, \tag{A2}$$

where $\mathbf{I}$ is the unit tensor and $\hat{r}$ is a unit vector along $\mathbf{r}$. We recall the definition of U_m^∞ in its time-independent version, *viz.,*

$$U_m^\infty(\mathbf{u}_1, \mathbf{u}_2) = \int_0^{r_C}\int_0^{\pi}\int_0^{2\pi} U_{\rm int}(\mathbf{r}, \mathbf{u}_1, \mathbf{u}_2) G_\infty(\mathbf{r}) r^2 \sin\vartheta_r \, dr \, d\vartheta_r \, d\varphi_r, \tag{A3}$$

where (ϑ_r, φ_r) are the spherical polar angles specifying the orientation of $\mathbf{r}$ and r_C is the radius of the minimal volume $\upsilon_{\min}$ of the cavity given by

$$r_C(T) = \left(\frac{3}{2\pi\rho_0(T)}\right)^{1/3}.$$

We expand G_∞ in spherical harmonics so that

$$G_\infty(\mathbf{r}) = \sum_{n=0}^{\infty}\sum_{m=-n}^{n} g^{n,m}(r)Y_{n,m}(\hat{r}) \tag{A4}$$

so that Eq. (A3) becomes

$$U_m^\infty(\mathbf{u}_1,\mathbf{u}_2) = \frac{\mu^2}{4\pi\varepsilon_0}\mathbf{u}_1\cdot\sum_{n=0}^{\infty}\sum_{m=-n}^{n}\int_0^{r_C} dr\frac{g^{n,m}(r)}{r}\int_0^{\pi}\int_0^{2\pi}\mathbf{T}(\hat{r})Y_{n,m}(\hat{r})\sin\vartheta_r\, d\vartheta_r\, d\varphi_r\cdot\mathbf{u}_2. \tag{A5}$$

It is obvious that only $n = 2$ terms will contribute to the double sum in Eq. (A5). Therefore, we have

$$U_m^\infty(\mathbf{u}_1,\mathbf{u}_2) = \frac{\mu^2}{4\pi\varepsilon_0}\mathbf{u}_1\cdot\sum_{m=-2}^{2}\int_0^{r_C} dr\frac{g^{2,m}(r)}{r}\int_0^{\pi}\int_0^{2\pi}\mathbf{T}(\hat{r})Y_{2,m}(\hat{r})\sin\vartheta_r\, d\vartheta_r\, d\varphi_r\cdot\mathbf{u}_2. \tag{A6}$$

Because G_∞ is real, we must have

$$g^{n,-m}(r) = (-1)^m\bar{g}^{n,m}(r), \tag{A7}$$

where only the overbar denotes the complex conjugate. Separating real and imaginary parts in $g^{n,m}(r)$, we write

$$g^{n,m}(r) = g'^{(n,m)}(r) + ig''^{(n,m)}(r) \tag{A8}$$

so that Eq. (A6) reads

$$\begin{aligned}U_m^\infty(\mathbf{u}_1,\mathbf{u}_1) = \frac{\mu^2}{4\pi\varepsilon_0}\Bigg\{&-4\sqrt{\frac{\pi}{5}}G_{20}\left[u_{1,Z}u_{2,Z}-\frac{1}{2}(u_{1,X}u_{2,X}+u_{1,Y}u_{2,Y})\right]+2\sqrt{\frac{6\pi}{5}}G'_{21}(u_{1,X}u_{2,Z}+u_{1,Z}u_{2,X})\\&-2\sqrt{\frac{6\pi}{5}}G''_{21}(u_{1,Y}u_{2,Z}+u_{1,Z}u_{2,Y})-2\sqrt{\frac{6\pi}{5}}G'_{22}(u_{1,X}u_{2,X}+u_{1,Y}u_{2,Y})+2\sqrt{\frac{6\pi}{5}}G''_{22}(u_{1,X}u_{2,X}+u_{1,Y}u_{2,Y})\Bigg\},\end{aligned}$$

where

$$G'_{nm} = \int_0^{r_C} g'^{(n,m)}(r)d(\ln r), \tag{A9}$$

$$G''_{nm} = \int_0^{r_C} g''^{(n,m)}(r)d(\ln r) \tag{A10}$$

are both *converging* integrals for r_C positive and finite.

Now, we come to modeling dipole-dipole interactions, because, we insist, solving the general problem is a very difficult one [13]. In order to model dipole-dipole interactions, let us consider the terms in Eq. (A9). To this purpose, we assume that the electric field is applied along the Z axis of the laboratory frame so that $\mathbf{e} = \hat{Z}$. We largely anticipate below that U_m^∞ as given by Eq. (A9) will occur under the integral sign in Eq. (3) so that the "=" in the following equations mean "has the same effect as" and does not represent an equality in the strict mathematical sense. The term proportional to G_{20} may be written $(\mathbf{u}\cdot\mathbf{e} = u_Z)$

$$u_{1,Z}u_{2,Z} - \tfrac{1}{2}(u_{1,X}u_{2,X}+u_{1,Y}u_{2,Y}) = (\mathbf{u}_1\cdot\mathbf{e})(\mathbf{u}_2\cdot\mathbf{e}) - \tfrac{1}{2}(\mathbf{u}_1\cdot\mathbf{u}_2 - (\mathbf{u}_1\cdot\mathbf{e})(\mathbf{u}_2\cdot\mathbf{e})) \tag{A11}$$

$$= \tfrac{3}{2}(\mathbf{u}_1\cdot\mathbf{e})(\mathbf{u}_2\cdot\mathbf{e}) - \tfrac{1}{2}(\mathbf{u}_1\cdot\mathbf{u}_2) \tag{A12}$$

$$= \tfrac{3}{2}(\mathbf{u}_1\cdot\mathbf{e})(\mathbf{u}_2\cdot\mathbf{e}) - \tfrac{3}{2}(\mathbf{u}_1\cdot\mathbf{e})(\mathbf{u}_2\cdot\mathbf{e}) \tag{A13}$$

$$= 0. \tag{A14}$$

Hence, the term proportional to G_{20} does not contribute to the dielectric constant. The terms proportional to G'_{21} and G''_{21} involve products between different dipole components. Since the field is directed along the Z axis, these terms have no effect. Therefore these terms drop out because they are useless. Most interesting are the terms proportional to G'_{22} and G''_{22}. Both invoke dipolar components that are perpendicular to the externally applied electric field. With the same meaning for the "=" sign as in Eq. (A14), we have

$$u_{1,X}u_{2,X} + u_{1,Y}u_{2,Y} = \mathbf{u}_1\cdot\mathbf{u}_2 - (\mathbf{u}_1\cdot\mathbf{e})(\mathbf{u}_2\cdot\mathbf{e}) = 3(\mathbf{u}_1\cdot\mathbf{e})(\mathbf{u}_2\cdot\mathbf{e}) - (\mathbf{u}_1\cdot\mathbf{e})(\mathbf{u}_2\cdot\mathbf{e}) \tag{A15}$$

$$= 2(\mathbf{u}_1\cdot\mathbf{e})(\mathbf{u}_2\cdot\mathbf{e}) \tag{A16}$$

so that U_m^{∞} becomes, using all the above results (and restoring the usual meaning for the "=" sign)

$$U_m^{\infty}(\mathbf{u}_1, \mathbf{u}_2) = \frac{\mu^2}{\varepsilon_0}\sqrt{\frac{6}{5\pi}}(\mathbf{u}_1 \cdot \mathbf{e})(\mathbf{u}_2 \cdot \mathbf{e}) \int_0^{r_C} [g''^{(2,2)}(r) - g'^{(2,2)}(r)]\, d(\ln r). \tag{A17}$$

We may compare this expression with Berne's equation for U_m^{∞} which is [44,58,61]

$$U_m^{\infty}(\mathbf{u}_1, \mathbf{u}_2) = \pm\frac{\rho_0 \mu^2}{3\varepsilon_0}(\mathbf{u}_1 \cdot \mathbf{e})(\mathbf{u}_2 \cdot \mathbf{e}), \tag{A18}$$

the $\pm$ sign being present because the integral in Eq. (A17) may be positive or negative, depending on the microstructure of the liquid [17]. This leads to a transcendent equation for ρ_0, *viz.*,

$$\rho_0 = \sqrt{\frac{54}{5\pi}} \left| \int_0^{\left(\frac{3}{2\pi\rho_0}\right)^{1/3}} [g''^{(2,2)}(r) - g'^{(2,2)}(r)]\, d(\ln r) \right|, \tag{A19}$$

and hence Eq. (15) results. The above equation explicitly shows, as was stated in Ref. [17], that the microstructure of the polar fluid is hidden in ρ_0.

[1] P. Debye, *Polar Molecules* (Dover, New York, 1929).
[2] C. J. F. Böttcher, *Theory of Electric Polarization*, Vol. I (Elsevier, Amsterdam, 1973).
[3] B. K. P. Scaife, *Principles of Dielectrics* (Clarendon, Oxford, 1998).
[4] L. Onsager, J. Am. Chem. Soc. **58**, 1486 (1936).
[5] J. G. Kirkwood, J. Chem. Phys. **7**, 911 (1939).
[6] H. Fröhlich, *Theory of Dielectrics* (Oxford University Press, Oxford, 1958).
[7] H. Fröhlich, *Theory of Dielectrics: Dielectric Constant and Dielectric Loss* (Clarendon Press, Oxford, 1949).
[8] G. Nienhuis and J. Deutch, J. Chem. Phys. **55**, 4213 (1971).
[9] M. S. Wertheim, J. Chem. Phys. **55**, 4291 (1971).
[10] G. Stell, G. N. Patey and J. Høye, Adv. Chem. Phys. **48**, 183 (1981).
[11] S. L. Carnie and G. N. Patey, Mol. Phys. **47**, 1129 (1982).
[12] P. Madden and D. Kivelson, Adv. Chem. Phys. **56**, 467 (1984).
[13] P. M. Déjardin, Phys. Rev. E **105**, 024109 (2022).
[14] M. Abramowitz and I. Stegun, *Handbook of Mathematical Functions* (Dover, New York, 1972).
[15] D. A. Varshalovich, A. N. Moskalev, and V. K. Khersonskii, *Quantum Theory of Angular Momentum* (World Scientific, Singapore, 1988).
[16] P. M. Déjardin, S. V. Titov, and Y. Cornaton, Phys. Rev. B **99**, 024304 (2019).
[17] P. M. Déjardin, Y. Cornaton, P. Ghesquière, C. Caliot, and R. Brouzet, J. Chem. Phys. **148**, 044504 (2018).
[18] A. Stone, *The Theory of Intermolecular Forces* (Oxford University Press, Oxford, 2013).
[19] C. Wohlfarth, *Static Dielectric Constants of Pure Liquids and Binary Mixtures* (Springer-Verlag, Berlin, 2008).
[20] M. Gussoni, R. Rui, and G. Zerbi, J. Mol. Struct. **447**, 163 (1998).
[21] R. D. Nelson Jr, D. R. Lide and A. A. Maryott, *Selected Values of Electric Dipole Moments for Molecules in the Gas Phase* (National Bureau of Standards, Washington, DC, 1967).
[22] J. Malecki, J. Nowak, and S. Balanicka, J. Phys. Chem. **88**, 4148 (1984).
[23] D. M. Petkovic, B. A. Kezele, and D. R. Rajic, J. Phys. Chem. **77**, 922 (1973).
[24] Dortmund Data Bank, www.ddbst.com (2020).
[25] J. Ortega, J. Chem. Eng. Data **27**, 312 (1982).
[26] T. E. Daubert, R. P. Danner, H. M. Sibel, and C. C. Stebbins, *Physical and Thermodynamic Properties of Pure Chemicals: Data Compilation* (Taylor and Francis, Washington, DC, 1997).
[27] Ch. Boned, A. Baylaucq, and J. Bazile, Fluid Phase Equilibr. **270**, 69 (2008).
[28] F. Alaoui, E. Montero, J. Bazile, M. Comuñas, and C. Boned, Fluid Phase Equilibr. **320**, 43 (2012).
[29] F. Alaoui, E. Montero, G. Qiu, F. Aguilar, and J. Wu, J. Chem. Thermodyn. **65**, 174 (2013).
[30] C. W. Ye and J. Li, Russ. J. Phys. Chem. A **86**, 1515 (2012).
[31] J. Mazur, Nature (London) **127**, 893 (1931).
[32] H. Schläfer and W. Schaffernicht, Angew. Chem. **72**, 618 (1960).
[33] Q. Tian, and H. Liu, J. Chem. Eng. Data **52**, 892 (2007).
[34] I. V. Blazhnov, N. P. Malomuzh, and S. V. Lishchuk, J. Chem. Phys. **121**, 6435 (2004).
[35] J. K. Vij, W. G. Scaife, and J. H. Calderwood, J. Phys. D: Appl. Phys. **11**, 545 (1978).
[36] Z. Hu and J. D. Weeks, J. Phys. Chem. C **114**, 10202 (2010).
[37] D. P. Shelton, J. Chem. Phys. **144**, 234506 (2016).
[38] S. E. McLain, A. K. Soper, and A. K. Luzar, J. Chem. Phys. **124**, 074502 (2006).
[39] A. Stoppa, A. Nazet, R. Buchner, A. Thoman, and M. Walther, J. Mol. Liquids **212**, 963 (2015).
[40] S. Helambe, M. Lokhande, A. Kumbarkhane, S. Mehrota, and S. Doraiswamy, Pramana **44**, 405 (1995).
[41] A. Kumbarkhane, S. Helambe, M. Lokhande, S. Doraiswamy, and S. Mehrota, Pramana **46**, 91 (1996).
[42] J. K. Vij and F. Hufnagel, J. Phys. Chem. **95**, 6142 (1991).
[43] T. Shikata, Y. Sakai, and J. Watanabe, AIP Adv. **4**, 067130 (2014).
[44] P. M. Déjardin and F. Ladieu, J. Chem. Phys. **140**, 034506 (2014).
[45] M. W. Evans, G. J. Evans, W. T. Coffey, and P. Grigolini, *Molecular Dynamics and the Theory of Broadband Spectroscopy* (Wiley, New York, 1982).
[46] P. M. Déjardin, W. T. Coffey, F. Ladieu, and Yu. P. Kalmykov, in *Nonlinear Dielectric Spectroscopy*, edited by R. Richert (Springer, Berlin, 2018), pp. 35–74.

[47] D. Matyushov and R. Richert, J. Chem. Phys. **144**, 041102 (2016).
[48] G. Oster and J. G. Kirkwood, J. Chem. Phys. **11**, 175 (1943).
[49] N. E. Hill, J. Phys. C **3**, 238 (1970).
[50] P. M. Déjardin and Y. Cornaton, J. Phys.: Conf. Series **1322**, 012039 (2019).
[51] D. Van der Spoel, P. J. Van Maaren, and H. J. C. Berendsen, J. Chem. Phys. **108**, 10220 (1998).
[52] F. Pabst, A. Helbling, J. Gabriel, P. Weigl, and T. Blochowicz, Phys. Rev. E **102**, 010606(R) (2020).
[53] M. Saini, Y. Guo, T. Wu, K. Ngai, and L. Wang, J. Chem. Phys. **149**, 204505 (2018).
[54] G. P. Johari and W. Dannhauser, J. Phys. Chem. **72**, 3273 (1968).
[55] W. Dannhauser, J. Chem. Phys. **48**, 1911 (1968).
[56] W. T. Coffey and Yu. P. Kalmykov, *The Langevin Equation*, 4th ed. (World Scientific, Singapore, 2017).
[57] H. Risken, *The Fokker-Planck Equation*, 2nd ed. (Springer, Berlin, 1989).
[58] P. M. Déjardin, J. Appl. Phys. **110**, 113921 (2011).
[59] B. Bagchi and A. Chandra, Adv. Chem. Phys. **80**, 1 (1991).
[60] M. te Vrugt, H. Löwen, and R. Wittkowski, Adv. Phys. **69**, 121 (2020).
[61] B. J. Berne, J. Chem. Phys. **62**, 1154 (1975).